Sains Malaysiana 43(2)(2014): 253–259

Effect of Monoethanolamine Loading on the Physicochemical Properties of Amine-Functionalized Si-MCM-41

(Kesan Penambahan Monoetanolamina terhadap Sifat Fiziko Kimia Si-MCM-41 Difungsikan oleh Amina)

ANITA RAMLI*, SOHAIL AHMED & SUZANA YUSUP

ABSTRACT

Siliceous mesoporous molecular sieve (Si-MCM-41) material with highly ordered hexagonal pore arrangement was synthesized at 373 K for 8-days duration by hydrothermal method, dried at 393 K and calcined at 823 K in N_2 atmosphere. The calcined Si-MCM-41 was later functionalized with 10-50 wt. % monoethanolamine (MEA) by impregnation method and dried in vacuum at 343 K. The MEA-Si-MCM-41 samples were characterized for their physicochemical properties with FTIR, XRD, TGA, HRTEM, FESEM, BET and elemental analysis. XRD results showed that the intensity of the characteristic peaks of Si-MCM-41 reduces with increasing loading of MEA indicating that the MEA molecules are loaded in the pores as well as on the surface of Si-MCM-41. The appearance of FTIR peaks corresponding to N-H, C-N and C-H bonds suggested that Si-MCM-41 has been functionalized with MEA. The presence of Si-O-Si peaks in FTIR spectra of MEA-Si-MCM-41 samples indicates that the hexagonal pore arrangement remains intact and this is supported by HRTEM images. FESEM images show that MEA-Si-MCM-41 samples became agglomerated with increase loading of MEA. TGA analyses show that the MEA-Si-MCM-41 samples are thermally stable up to 528 K. N_2 adsorption-desorption isotherms show that the textural properties of Si-MCM-41 material slowly change from a mesoporous material to non-porous material as the MEA loading increases due to pore filling effect during functionalization with MEA. Detection of N, C and H by elemental analysis confirms the presence of MEA in MEA-Si-MCM-41 samples.

Keywords: Functionalization; MEA; physicochemical properties; Si-MCM-41

ABSTRAK

Bahan penapis molekul berliang meso berasaskan silika (Si-MCM-41) dengan struktur liang secara heksagon yang sangat tersusun telah disintesis pada suhu 373 K selama 8 hari menggunakan kaedah hidroterma, dikeringkan pada 393 K dan dikalsinkan pada 823 K dalam aliran N_2. Si-MCM-41 yang telah dikalsinkan kemudiannya difungsikan dengan memuatkan 10-50 wt. % monoetanolamina (MEA) ke dalam liangnya menggunakan kaedah pengisitepuan dan dikeringkan menggunakan vakum pada suhu 343 K. Sifat fiziko kimia sampel MEA-Si-MCM-41 telah dianalisis dengan menggunakan FTIR, XRD, TGA, TEM, FESEM, BET dan analisis unsur. Keputusan XRD menunjukkan bahawa keamatan puncak Si-MCM-41 berkurangan dengan peningkatan muatan MEA menunjukkan bahawa molekul MEA telah dimuatkan ke dalam liang serta pada permukaan Si-MCM-41. Kehadiran puncak FTIR yang sepadan dengan ikatan N-H, C-N dan C-H mencadangkan bahawa Si-MCM-41 telah difungsikan oleh MEA. Kehadiran puncak Si-O-Si pada spektra FTIR bagi sampel MEA-Si-MCM-41 menunjukkan bahawa struktur liang secara heksagon masih utuh dan ini disokong oleh mikrograf HRTEM. Mikrograf FESEM menunjukkan bahawa sampel MEA-Si-MCM-41 menjadi bergumpal dengan peningkatan muatan MEA. Analisis TGA menunjukkan bahawa sampel MEA-Si-MCM-41 mempunyai kestabilan terma sehingga suhu 528 K. Isoterma penjerapan-penyahjerapan menunjukkan bahawa sifat tekstur bahan Si-MCM-41 berubah secara perlahan daripada bahan berliang meso kepada bahan tidak berliang setelah muatan MEA meningkat disebabkan kesan pengisian liang semasa pemfungsian dengan MEA. Pengesanan N, C dan H melalui analisis unsur mengesahkan kehadiran MEA di dalam sampel MEA-Si-MCM-41.

Kata kunci: MEA; pemfungsian; sifat fiziko kimia; Si-MCM-41

INTRODUCTION

MCM-41 is a mesoporous molecular sieve with hexagonal pore structure, uniform pore size over micrometer length scales and tunable pore size in the range of 15-100 Å (Beck et al. 1992; Kresge et al. 1992). It generally has surface area of greater than 700 m^2/g and pore volume of at least 0.7 cm^3/g. The MCM-41 has high thermal and hydrothermal stability, large number of hydroxyl (silanol) groups (~40-60%) and ease of surface modification (Beck et al. 1992; Cheng et al. 1995; Jiang et al. 2008). These remarkable properties make this material attractive for applications as catalyst/catalyst support (Corma et al. 1995; Nazari et al. 2005), adsorption and separation (Belmabkhout et al. 2009; Rathousky et al. 1995), ion-exchange (Kim et al. 1995) and environmental safety (Feng et al. 1997).

Due to the remarkable characteristics of the MCM-41 material, it has high potential as adsorbent for adsorption and separation of carbon dioxide (CO_2) gas. Pure MCM-41 has been reported to show low adsorption of CO_2 at ambient temperature and pressure (Belmabkhout et al. 2009) which may be due to the weak interaction between Si-MCM-41 and CO_2. Thus, it is important to improve its adsorption capacity for CO_2. Functionalization of mesoporous silica with polyethylenimine (PEI) has been reported to result in improvement of CO_2 adsorption capacity and selectivity (Bhagiyalakshmi et al. 2010; Son et al. 2008).

This paper reports on the functionalization of Si-MCM-41 with 10–50 wt. % MEA loading via impregnation method to study the effect of increasing MEA loading on the physicochemical properties of Si-MCM-41.

Materials and Methods

Si-MCM-41 was synthesized by hydrothermal method at 373 K for 8 days duration (Ramli et al. 2012). The synthesized Si-MCM-41 was functionalized with MEA via wet impregnation method similar to that reported by Ahmed et al. (2012). Typically, the required amount of MEA (Merck 99.9%) to give 10-50 wt. % loading was added to 10 g of methanol (Merck 99.9%) and stirred for 15 min for complete dissolution of MEA. Then, 2 g of the synthesized Si-MCM-41 were dispersed into the amine solution with vigorous stirring for 30 min and later dried at 343 K for 16 h in vacuum of 700 mm Hg. The resulted materials are denoted as X wt. % MEA-Si-MCM-41, where X represents the MEA loading in the sample.

The X-ray diffraction (XRD) analysis was performed on Bruker D8 Advance diffractometer using monochromated Cu Kα radiation (l = 1.541 Å). The scanning was performed in the 2θ = 1-10° region with 0.010° step size and 4 s step time. Fourier transformed infrared (FTIR) spectra was acquired on a SHIMADZU 8400S spectrometer in the 400-4000 cm^{-1} region. Surface morphology was investigated by variable pressure field emission scanning electron microscopy (VPFESEM) on ZEISS 55 Supra VP microscope operated at accelerated voltage of 5.00 kV and 30000 magnifications. HRTEM images were recorded using a Zeiss Libra 200FE transmission electron microscope operated at an acceleration voltage of 200 kV. Thermal gravimetric analysis was carried out using thermal gravimetric analyzer TG/DTA EXSTAR 6300 SII (Japan) where the temperature was increased linearly from 303 to 1273 K at a heating rate of 10 K/min in N_2 flow rate of 100 mL/min. Nitrogen adsorption-desorption measurements were carried out using Micromeritics ASAP 2020 analyzer with N_2 as the adsorbate at 77 K. Si-MCM-41 sample was degassed for 2 h at 523 K prior to the measurement while MEA-Si-MCM-41 was degassed for 4 h at 373 K. Total surface area was obtained by multipoint Brunauer–Emmet–Teller method (BET) (Brunauer et al. 1938) and average pore diameter was determined by the Barret–Joyner–Halenda (BJH) (Barrett et al. 1951) method from the desorption branch of the isotherm. Elemental analysis for the determination of C, H and N contents were carried out using a LECO CHNS-932 USA elemental analyzer.

Results and Discussion

In general, the diffractogram of pure Si-MCM-41 displays a unique three or four diffraction peaks in the 2θ = 1–10° region, which are also known as its fingerprints (Beck et al. 1994). The diffractograms of all samples are shown in Figure 1. Si-MCM-41 shows four diffraction peaks with a very sharp peak at ~2.1° which is assigned to (100) plane and three weaker peaks at 2θ = ~3.6, ~4.1 and ~5.5° which are assigned to (110), (200) and (210) planes, respectively.

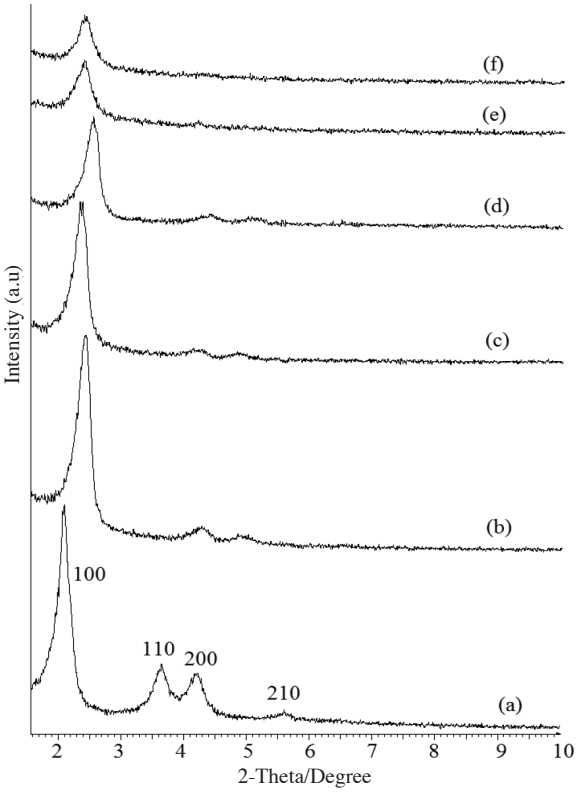

FIGURE 1. XRD diffractograms of (a) Si-MCM-41 (b) 10 wt. % (c) 20 wt. % (d) 30 wt. % (e) 40 wt. % and (f) 50 wt. % MEA-Si-MCM-41

The presence of these distinct peaks in the XRD diffractogram confirm that the synthesized Si-MCM-41 has uniform hexagonal shape pore arrangement (Beck et al. 1992). The appearance of peaks above 2θ = 3° shows that the material has fine long range order mesopores (Chuah et al. 2002), while lack of these peaks suggested the presence of disordered structure in the Si-MCM-41 (Blin et al. 2001). The unique characteristics of Si-MCM-41 is that it exhibits diffraction peaks only at low 2θ values indicating that arrangement of the atoms within the walls is essentially amorphous (Chuah et al. 2002).

The intensity of X-ray diffraction peaks of functionalized Si-MCM-41 materials depends on the type

of material present in the pores and the scattering power of the host material. Low density material leads to an intense (100) diffraction peak while the material with highest density would generate a very weak (100) reflection. The changes in the intensity of the X-ray diffraction peaks of MEA-Si-MCM-41 are due to the difference in the scattering contrast between two building blocks of the MCM-41 structure (i.e. amorphous silicate wall and MEA as the filling material). In general, the intensity of the X-ray peaks decreases with decreasing scattering contrast and is zero when the scattering power of the silicate wall and the pore filling material are similar (Marler et al. 1996).

The intensity of the diffraction peaks in MEA-Si-MCM-41 samples decreases considerably as the MEA loading increases and the peaks above $2\theta = 3^{o}$ finally disappeared as the MEA loading reaches 50 wt. %. This may be due to a decrease in the scattering contrast of the silicate wall and the MEA present in the pores. The disappearance of the peaks at higher 2θ values is due to pore filling and successive structural construction of MEA with Si-MCM-41 (Bhagiyalakshmi et al. 2010). It is also noted that the diffraction peaks of MEA-Si-MCM-41 samples shifted slightly towards higher 2θ values. These observations indicate the successful loading of MEA either into the pore channels or on the surface of the Si-MCM-41 (Son et al. 2008; Xu et al. 2002).

FTIR spectra of all samples are shown in Figure 2. FTIR spectra of Si-MCM-41 shows the presence of a broad peak in the 3100-3700 cm^{-1} region which is attributed to –OH stretching of surface silanol groups (Si-OH) and adsorbed water molecules while a peak at ~1635 cm^{-1} represents the bending vibration of the adsorbed water molecules (H-O-H). The symmetric and asymmetric stretching of Si-O in Si-O-Si are represented by the peak at ~1080 cm^{-1} with a shoulder at ~1240 cm^{-1} and accompanied by a peak at 794 cm^{-1}. The characteristic peak of Si-MCM-41 appears at ~964 cm^{-1} which is corresponding to the stretching of $Si\text{-}O^{-}$ (Si-OH) present on the surface of the mesoporous material (Grisdanurak et al. 2003; Jiang et al. 2008; Liu et al. 2004; Romero et al. 1997).

Noticeable changes are observed after functionalization of the Si-MCM-41 with MEA. The intensity of the peaks at ~3450 and ~1635 cm^{-1} which are due to -OH stretching and bending vibrations first reduces when the MEA loading was increased to 20 wt. % but later the intensity of the peaks increases as the MEA loading was increased. At lower loading of MEA, the intensity of these peaks reduces due to the attachment of MEA to the surface silanol group in the hexagonal channels. Once the pores are filled with MEA, excess MEA would be deposited on the outer surface of Si-MCM-41 which enables its detection, thus increases the intensity of the peaks correspond to -OH stretching and bending vibrations.

The intensity of the characteristic peak at 964 cm^{-1} due to Si-O-H bending of silanol groups decreases gradually and finally disappeared as the MEA loading was increased to 50 wt. %. This suggests that there is a chemical interaction

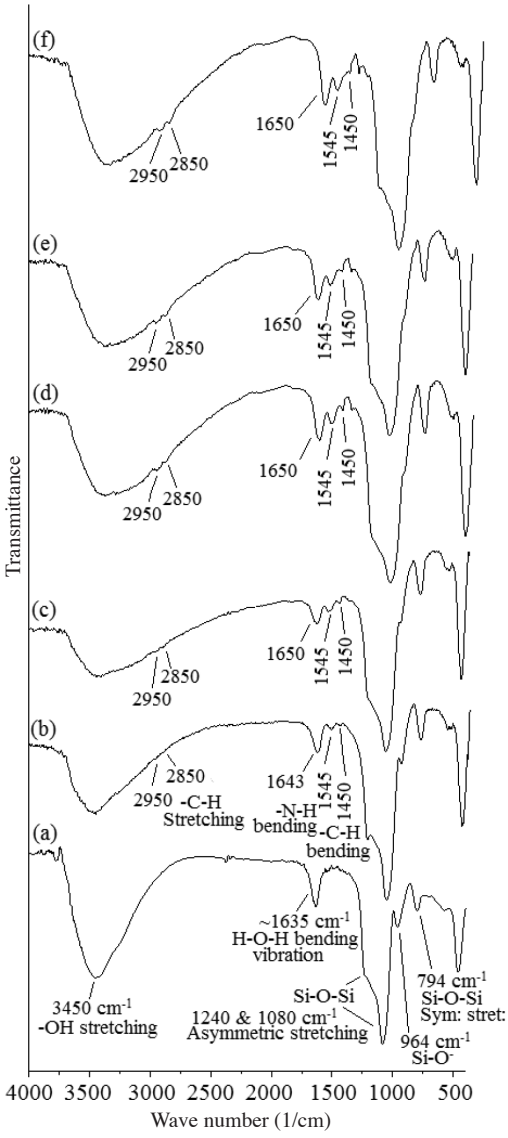

FIGURE 2. FTIR spectra (a) Si-MCM-41 (b) 10 wt. % (c) 20 wt. % (d) 30 wt. % (e) 40 wt. % and (f) 50 wt. % MEA-Si-MCM-41

between the silanol groups on the surface of the Si-MCM-41 and the amine groups of MEA, which may form $Si\text{-}O^{-}N^{+}H_2R$ or $Si\text{-}O^{-}N^{+}HR$ interaction. Such chemical interaction works as an anchor on the surface of MCM-41 and keeps MEA in the pore channels (Ma et al. 2009). These sites may act as active sites for CO_2 adsorption (Drage et al. 2008; Son et al. 2008).

The intensity of the peaks at ~1450, ~1550 and ~1315 cm^{-1} which are corresponding to C-H bending, N-H or NH_2 bending (Bhagiyalakshmi et al. 2010; Drage et al. 2008) and -C-N vibration, respectively, increases as the MEA loading increases. The intensity of the peaks at ~2850 and ~2960 cm^{-1} corresponding to C-H stretching associated with MEA also increases gradually as the MEA loading increases (Yue et al. 2008). These peaks were absent in the pure Si-MCM-41 sample and only detected in MEA-Si-MCM-41 samples, hence confirms that Si-MCM-41 has been functionalized with MEA.

Surface morphology of Si-MCM-41 and MEA-Si-MCM-41 are shown in Figure 3. FESEM micrograph of pure Si-MCM-41 shows that Si-MCM-41 is composed of spherical particles along with irregular shaped particles in the form of agglomerates of different sizes. During functionalization of Si-MCM-41 with MEA, the MEA molecules were first deposited into the pores. When the pores are filled with MEA molecules, excess MEA would be deposited on the outer surface resulting in agglomeration of the mesoporous material. Figure 3(e) - 3(f) shows that there are many large external pores between the particles, which will improve the diffusion of gas molecules from bulk gas phase to the surface of the material (Ma et al. 2009).

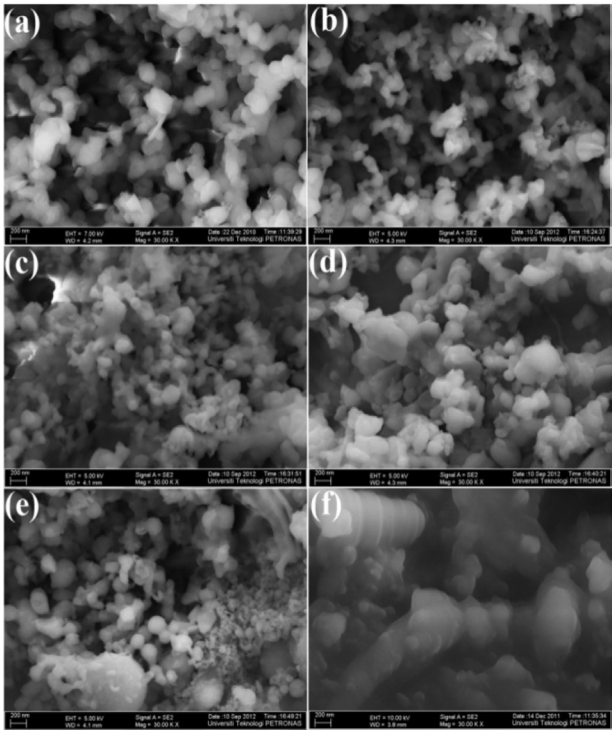

FIGURE 3. Morphology of (a) Si-MCM-41 (b) 10 wt. % (c) 20 wt. % (d) 30 wt. % (e) 40 wt. % and (f) 50 wt. % MEA-Si-MCM-41

HRTEM images of Si-MCM-41 and MEA-Si-MCM-41 are shown in Figure 4. It can be seen that Si-MCM-41 is a highly ordered material with uniformly arranged pores of hexagonal shape or also known as honeycomb-like structure. The HRTEM images of MEA-Si-MCM-41 samples show noticeable uniform pores of hexagonal shape which indicate that the pore arrangement remains intact even after functionalization with MEA.

TGA profiles of MEA-Si-MCM-41 samples are shown in Figure 5. In general, three steps of weight loss were observed. The first step is observed at temperatures between 308–443 K which is due to removal of adsorbed moisture from the samples followed by a sharp weight loss between 423–688 K which may be attributed to the volatilization and degradation of MEA as its boiling point is 443 K and finally a gradual weight loss between 663-

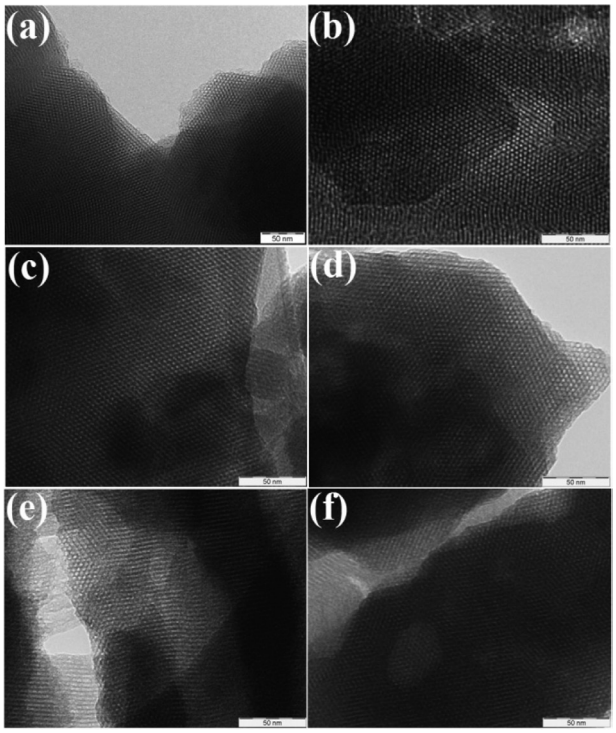

FIGURE 4. HRTEM images of (a) Si-MCM-41 (b) 10 wt. % (c) 20 wt. % (d) 30 wt. % (e) 40 wt. % and (f) 50 wt. % MEA-Si-MCM-41

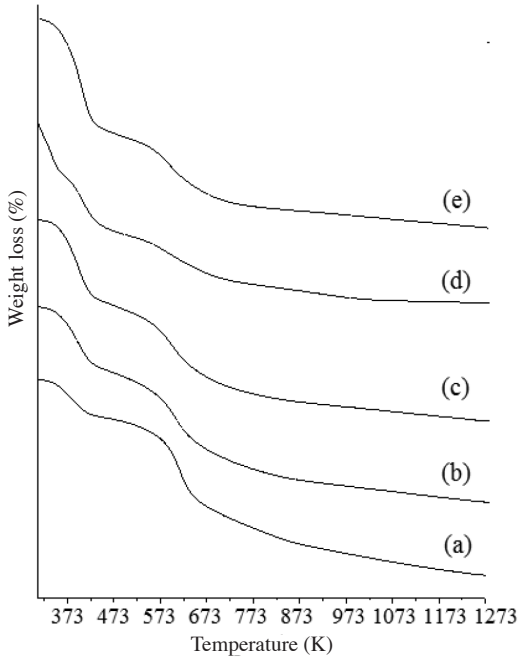

FIGURE 5. TGA profiles of samples (a) 10 wt. % (b) 20 wt. % (c) 30 wt. % (d) 40 wt. % and (e) 50 wt. % MEA-Si-MCM-41

1273 K. It is also observed that the thermal stability of MEA-Si-MCM-41 decreases as the MEA loading increases which could be attributed to the uniform distribution of MEA in the mesopores and on the outer surface of the MEA-Si-MCM-41.

Table 1 shows the degradation temperature of the MEA-Si-MCM-41 samples. As the MEA loading was increased, the sharp weight loss due to degradation of MEA occurred progressively at lower temperatures. This suggests that at low loading most of the MEA molecules are strongly bonded to the silanol groups in a monolayer and bi-layer forms thus will degrade at higher temperature. However, as the MEA loading increases, these molecules are loaded in a multi-layer form, hence most of the MEA molecules are weakly bonded to the silanol group and hence they are easier to degrade.

Figure 6 shows the N_2 adsorption-desorption isotherms of all samples. Si-MCM-41 shows Type IV isotherm according to the IUPAC classification which is a characteristics of a mesoporous material (Liu et al. 2004; Sing et al. 1985). Functionalization of Si-MCM-41 with MEA resulted in pore filling of the mesoporous material as the MEA loading was increased from 10-50 wt. %. This is indicated by progressive changes in the isotherm to Type III isotherm which is the characteristics of a non-porous material. The decrease in surface area, average pore size and total pore volume of the MEA-Si-MCM-41 samples with an increase in MEA loading (Table 2) are in accordance with pore filling effect by MEA which have been observed in XRD, FESEM and HRTEM analysis. Since the N_2 adsorption-desorption isotherms show that MEA-Si-MCM-41 loaded with 40 and 50 wt. % MEA are non-porous material (Type III material), these materials are considered as not having pore size or the pore size is negligible, since the pores have been filled by MEA molecules, as shown in Table 2.

TABLE 1. Weight loss temperature ranges of MEA functionalized MCM-41 samples

Sample	Moisture removal (K)	MEA decomposition		Sharp weight loss (K)
		Weakly bonded (K)	Strongly bonded (K)	
10 wt. % MEA-Si-MCM-41	308-423	423-663	663-1273	573
20 wt. % MEA-Si-MCM-41	308-428	428-668	668-1273	543
30 wt. % MEA-Si-MCM-41	308-433	433-673	673-1273	538
40 wt. % MEA-Si-MCM-41	308-438	438-683	683-1273	533
50 wt. % MEA-Si-MCM-41	308-443	443-688	688-1273	528

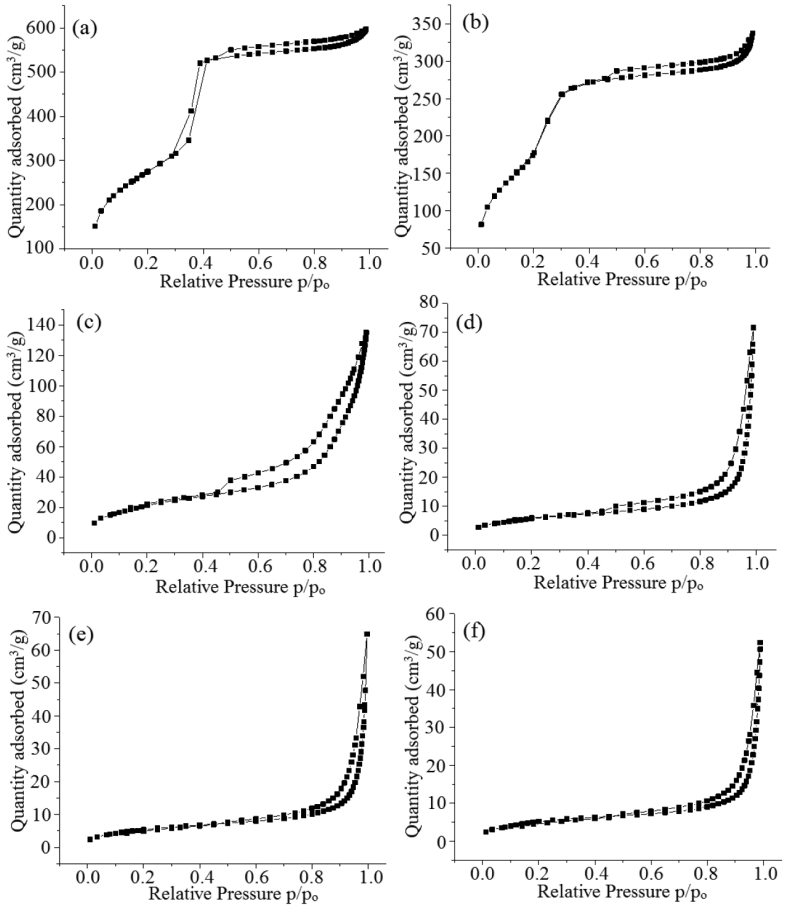

FIGURE 6. Adsorption-desorption isotherms of (a) Si-MCM-41 (b) 10 wt. % (c) 20 wt. % (d) 30 wt. % (e) 40 wt. % (f) 50 wt. % MEA-Si-MCM-41

TABLE 2. Textural properties of Si-MCM-41 and MEA-Si-MCM41

Sample	Surface area (m^2/g)	Pore volume (cm^3/g)	Pore diameter (nm)
Si-MCM-41	993	1.009	3.1
10 wt. % MEA Si-MCM-41	748	0.590	2.2
20 wt. % MEA Si-MCM-41	81	0.214	2.1
30 wt. % MEA Si-MCM-41	22	0.112	1.9
40 wt. % MEA Si-MCM-41	20	0.102	--
50 wt. % MEA Si-MCM-41	19.81	0.082	--

TABLE 3. Theoretical and experimental values of C, H and N content in MEA-Si-MCM-41

Samples wt. % MEA-MCM-41	Experimental contents (%)			Theoretical contents (%)		
	C	H	N	C	H	N
10 wt. % MEA Si-MCM-41	3.99	5.51	2.60	3.93	1.15	2.29
20 wt. % MEA Si-MCM-41	6.76	2.70	4.00	7.87	2.31	4.58
30 wt. % MEA Si-MCM-41	9.30	2.52	5.18	11.80	3.46	6.88
40 wt. % MEA Si-MCM-41	10.75	2.99	5.74	15.73	4.62	9.17
50 wt. % MEA Si-MCM-41	12.58	3.51	6.50	19.66	5.77	11.46

Table 3 shows the C, H and N content in MEA-Si-MCM-41 samples as determined by CHNS elemental analyzer and the values are compared with the theoretical content. Theoretical content of C, H and N were calculated from the actual amount of MEA used for functionalization. The C, H and N content in MEA-Si-MCM-41 were found to increase with increasing loading of MEA which are in good agreement with the theoretical values. However, the deviation from the theoretical values became greater at higher loading of MEA which may indicate that not all MEA were loaded into the pores and on the outer surface of Si-MCM-41.

CONCLUSION

Si-MCM-41 was functionalized with 10-50 wt. % MEA via impregnation method. The intensity of diffraction peaks attributed to Si-MCM-41 fingerprints decreases with increasing loading of MEA due to pore filling and attachment of MEA on the external surface of Si-MCM-41. The presence of characteristic peaks at 794, 1080 and 1240 cm^{-1} in the FTIR spectra show that the Si-MCM-41 framework remains intact after functionalization and this is supported by HRTEM images. Appearance of new FTIR peaks at 1450, 1545, 2850 and 2960 cm^{-1} and detection of C, H and N by elemental analysis on the MEA-Si-MCM-41 confirm that Si-MCM-41 has been successfully functionalized with MEA. Thermal stability of the MEA-Si-MCM-41 decreases with increasing loading of MEA. The textural properties of Si-MCM-41 changes from mesoporous to non-porous material due to pore filling effect by the MEA but the hexagonal pore shapes remain intact.

ACKNOWLEDGEMENTS

The authors are grateful for the funding provided by the Ministry of Education (MOE) Malaysia under Fundamental Research Grant Scheme (FRGS/1/2012/SG01/UTP/02/02). The authors would also like to thank Universiti Teknologi PETRONAS for the Graduate Assistantship awarded to Mr Sohail Ahmed.

REFERENCES

Ahmed, S., Ramli, A. & Yusup, S. 2012. Effect of polyethylenimine loading on the physicochemical properties of amine-functionalized Si-MCM-41. *Malaysian Journal of Microscopy* 8: 22-27.

Barrett, E.P., Joyner, L.G. & Halenda, P.P. 1951. The determination of pore volume and area distributions in porous substances. I. Computations from Nitrogen isotherms. *Journal of the American Chemical Society* 73: 373-380.

Beck, J.S., Vartuli, J.C., Kennedy, G.J., Kresge, C.T., Roth, W.J. & Schramm, S.E. 1994. Molecular or supramolecular templating: Defining the role of surfactant chemistry in the formation of microporous and mesoporous molecular sieves. *Chemistry of Materials* 6: 1816-1821.

Beck, J.S., Vartuli, J.C., Roth, W.J., Leonowicz, M.E., Kresge, C.T., Schmitt, K.D., Chu, C.T.W., Olson, D.H. & Sheppard, E.W. 1992. A new family of mesoporous molecular sieves prepared with liquid crystal templates. *Journal of the American Chemical Society* 114: 10834-10843.

Belmabkhout, Y., Serna-Guerrero, R. & Sayari, A. 2009. Adsorption of CO2 from dry gases on MCM-41 silica at ambient temperature and high pressure. 1: Pure adsorption. *Chemical Engineering Science* 64: 3721-3728.

Bhagiyalakshmi, M., Yun, L., Anuradha, R. & Jang, H. 2010. Synthesis of chloropropylamine grafted mesoporous MCM-41, MCM-48 and SBA-15 from rice husk ash: Their application to CO_2 chemisorption. *Journal of Porous Materials* 17: 475-484.

Blin, J.L., Otjacques, C., Herrier, G. & Su, B.L. 2001. Kinetic study of MCM-41 synthesis. *International Journal of Inorganic Materials* 3: 75-86.

Brunauer, S., Emmett, P.H. & Teller, E. 1938. Adsorption of gases in multimolecular layers. *Journal of the American Chemical Society* 60: 309-319.

Cheng, C.F., Luan, Z. & Klinowski, J. 1995. The role of surfactant micelles in the synthesis of the mesoporous molecular sieve MCM-41. *Langmuir* 11: 2815-2819.

Chuah, G.K., Hu, X., Zhan, P. & Jaenicke, S. 2002. Catalysts from MCM-41: Framework modification, pore size engineering, and organic-inorganic hybrid materials. *Journal of Molecular Catalysis A: Chemical* 181: 25-31.

Corma, A., Martinez, A., Martinezsoria, V. & Monton, J.B. 1995. Hydrocracking of vacuum gasoil on the novel mesoporous MCM-41 Aluminosilicate catalyst. *Journal of Catalysis* 153: 25-31.

Drage, T.C., Arenillas, A., Smith, K.M. & Snape, C.E. 2008. Thermal stability of polyethylenimine based carbon dioxide adsorbents and its influence on selection of regeneration strategies. *Microporous and Mesoporous Materials* 116: 504-512.

Feng, X., Fryxell, G.E., Wang, L.Q., Kim, A.Y., Liu, J. & Kemner, K.M. 1997. Functionalized monolayers on ordered mesoporous supports. *Science* 276: 923-926.

Grisdanurak, N., Chiarakorn, S. & Wittayakun, J. 2003. Utilization of mesoporous molecular sieves synthesized from natural source rice husk silica to chlorinated volatile organic compounds (CVOCs) adsorption. *Korean Journal of Chemical Engineering* 20: 950-955.

Jiang, T., Lu, L., Yang, X., Zhao, Q., Tao, T., Yin, H. & Chen, K. 2008. Synthesis and characterization of mesoporous molecular sieve nanoparticles. *Journal of Porous Materials* 15: 67-73.

Kim, J.M., Kwak, J.H., Jun, S. & Ryoo, R. 1995. Ion exchange and thermal stability of MCM-41. *The Journal of Physical Chemistry* 99: 16742-16747.

Kresge, C.T., Leonowicz, M.E., Roth, W.J., Vartuli, J.C. & Beck, J.S. 1992. Ordered mesoporous molecular sieves synthesized by a liquid-crystal template mechanism. *Nature* 359: 710-712.

Liu, L., Zhang, G.Y. & Dong, J.X. 2004. Large pore mesoporous MCM-41 templated from Cetyltriethylammonium Bromide. *Chinese Chemical Letters* 15: 737-740.

Ma, X., Wang, X. & Song, C. 2009. Molecular basket sorbents for separation of CO2 and H2S from various gas streams. *Journal of the American Chemical Society* 131: 5777-5783.

Marler, B., Oberhagemann, U., Vortmann, S. & Gies, H. 1996. Influence of the sorbate type on the XRD peak intensities of loaded MCM-41. *Microporous Materials* 6: 375-383.

Nazari, K., Shokrollahzadeh, S., Mahmoudi, A., Mesbahi, F., Matin, N.S. & Moosavi-Movahedi, A.A. 2005. Iron(III) protoporphyrin/MCM41 catalyst as a peroxidase enzyme model: Preparation and typical test reactions. *Journal of Molecular Catalysis A: Chemical* 239: 1-9.

Ramli, A., Ahmed, S. & Yusup, S. 2012. Effect of synthesis duration on the physicochemical properties of siliceous mesoporous molecular sieve (Si-MMS). *Deffect and Diffusion Forum* 326-328: 647-653.

Rathousky, J., Zukal, A., Franke, O. & Schulz-Ekloff, G. 1995. Adsorption on MCM-41 mesoporous molecular sieves. Part 2. Cyclopentane isotherms and their temperature dependence. *Journal of the Chemical Society, Faraday Transactions* 91: 937-940.

Romero, A.A., Alba, M.A.D., Zhou, W. & Klinowski, J. 1997. Synthesis and characterization of the mesoporous silicate molecular sieve MCM-48. *The Journal of Physical Chemistry B* 101: 5294-5300.

Sing, K.S.W., Everett, D.H., Haul, R.A.W., Moscou, L., Pierotti, R.A., Rouquerol, J. & Siemieniewska, T. 1985. Reporting physisorption data for gas/solid systems with special reference to the determination of surface area and porosity. *Pure Appl. Chem.* 57: 603-609.

Son, W.J., Choi, J.S. & Ahn, W.S. 2008. Adsorptive removal of carbon dioxide using polyethyleneimine-loaded mesoporous silica materials. *Microporous and Mesoporous Materials* 113: 31-40.

Xu, X., Song, C., Andresen, J.M., Miller, B.G. & Scaroni, A.W. 2002. Novel polyethylenimine-modified mesoporous molecular sieve of MCM-41 type as high-capacity adsorbent for CO2 capture. *Energy & Fuels* 16: 1463-1469.

Yue, M.B., Sun, L.B., Cao, Y., Wang, Y., Wang, Z.J. & Zhu, J.H. 2008. Efficient CO_2 capturer derived from as-synthesized MCM-41 modified with amine. *Chemistry – A European Journal* 14: 3442-3451.

Anita Ramli*
Department of Fundamental and Applied Sciences
Universiti Teknologi PETRONAS
Bandar Seri Iskandar, 31750 Tronoh, Perak
Malaysia

Sohail Ahmed & Suzana Yusup
Department of Chemical Engineering
Universiti Teknologi PETRONAS
Bandar Seri Iskandar, 31750 Tronoh, Perak
Malaysia

*Corresponding author; email: anita_ramli@petronas.com.my

Received: 5 February 2013
Accepted: 26 July 2013